Proceedings of ALGORITMY 2024
pp. 204–213

GRAPH-LAPLACIAN IN BIODIVERSITY MODELLING BY NATURAL NUMERICAL NETWORKS*

ANETA A. OŽVAT†, MICHAL KOLLÁR†, MÁRIA ŠIBÍKOVÁ‡, AND KAROL MIKULA†

Abstract. This paper explores the graph-Laplacian operator and its application in image classification tasks, focusing on its effectiveness in capturing local variation and structural properties of data. We investigate its mathematical formulation, practical implementation, and usability in biodiversity modelling, extending Laplace operator application from the physical domain to graph structures. Our research proposes a novel methodology for identifying and classifying natural riparian forests with high biodiversity value from optical satellite imagery. We combine graph-Laplacian analysis with relevancy maps generated by the Natural Numerical Network to distinguish between natural and planted riparian forests. Furthermore, we explore graph-Laplacian as a statistical characteristic of Sentinel-2 optical bands in constructing the Natural Numerical Network. Numerical experiments and case studies highlight the applicability of the graph-Laplacian operator in environmental science, describing its potential in biodiversity modelling and protected habitat identification.

Key words. Laplace operator on the graphs, numerical methods, Natura 2000, natural riparian forests, planted forests, satellite images

AMS subject classifications. 35Q68, 35Q92, 35R02, 62H30

1. Introduction. The main aim of this paper is to explore the graph-Laplacian operator and its application in image classification tasks due to its effectiveness in capturing local variation and structural properties of data. In this paper, we investigate the mathematical formulation, practical implementation, and usability of the graph-Laplacian in biodiversity modelling. The graph-Laplacian extends the concept of the well-known Laplace operator in the context of the finite volume method in the 2D physical domain to graph structures, offering a potential tool for understanding complex data representations. The primary objective of this research is to propose a novel methodology for identifying and classifying natural riparian forests with high biodiversity value from satellite imagery using a combined approach of graph-Laplacian analysis and relevancy maps generated by the Natural Numerical Network (NatNet). Thus, natural riparian forests will be distinguished from planted riparian forests with low biodiversity value, which should not be part of the European Natura 2000 protected network [4]. Monitoring natural riparian forests and distinguishing them from planted riparian forests is essential because planted ones should not be a part of the Natura 2000 network. Additionally, we explore the graph-Laplacian as a statistical characteristic in constructing the graph structure of NatNet, enriching the spectrum of metrics used in data analysis and classification tasks, improving classification outcomes and delineating specific clusters with greater accuracy. Through numerical experiments and case studies, we highlight the applicability of the graph-Laplacian operator in environmental science.

*This work was supported by Grants APVV-19-0460, APVV-23-0186 and VEGA 1/0249/24.

†Department of Mathematics, Slovak University of Technology in Bratislava, Radlinského 11, 810 05 Bratislava, Slovakia, e-mail: ozvat@math.sk, kollarm@math.sk, mikula@math.sk.

‡Plant Science and Biodiversity Center, Slovak Academy of Sciences, Dúbravská cesta 9, 845 23 Bratislava, Slovakia, e-mail: maria.sibikova@savba.sk.

2. Natural Numerical Network. Inspired by work in ODE and PDE-based deep learning methods, particularly from [7, 3], the Natural Numerical Network was introduced as a novel supervised deep learning approach working on directed graphs [9]. NatNet is based on a forward-backward diffusion model on directed graphs, discretised numerically for image classification. It focuses on attraction-repulsion strategies, similar to those in high-dimensional data visualisation [2], and uses a nonlinear forward-backward diffusion equation for supervised classification as introduced in [8].

Let G be a directed graph consisting of a non-empty finite set $V(G)$ of vertices and a finite set $A(G)$ of ordered pairs of distinct vertices, called arcs or directed edges [1]. The number of vertices in G is denoted by N_V. For any arc $(u, v) = e_{uv}$, u is the tail, and v is the head, signifying departure from u and arrival at v [1]. Hereafter, we consider a semi-complete directed graph G, where every pair of vertices in $V(G)$ is connected by an arc.

Let $X : G \times [0, T] \to \mathbb{R}^k$ represent the Euclidean coordinates of vertex $v \in V(G)$ at time $t \in [0, T]$, given by $X(v, t) = (x_1(v, t), \ldots, x_k(v, t))$. The dimension of the feature space R^k is denoted by k. The diffusion of $X(v, t)$ on the graph G is described by the partial differential equation (PDE):

$$\partial_t X(v,t) = \nabla \cdot (g \nabla X(v,t)), \quad v \in V(G), \quad t \in [0,T], \tag{2.1}$$

where g represents the diffusion coefficient [6]. Equation (2.1) is considered together with the initial condition $X(v, 0) = X^0(v)$, $v \in V(G)$. Boundary conditions are unnecessary due to the semi-completeness of the graph G.

The diffusion coefficient g depends on the distance between vertices v and u in the graph G, leading to a nonlinear diffusion model. Specifically, $g(e_{uv})$ is formulated as:

$$g(e_{uv}) = \varepsilon(e_{uv}) \frac{1}{1 + \sum_{i=1}^{k} (K_i \; l_i^2(e_{uv}))}, \quad K_i \geq 0, \; i = 1, \ldots, k, \tag{2.2}$$

where K_i are weights for each coordinate $l_i(e_{uv})$, $i = 1, \ldots, k$, of the vector $l(e_{uv}) = (l_1(e_{uv}), \ldots, l_k(e_{uv}))^T = X(v, \cdot) - X(u, \cdot)$, allowing control over diffusion speed in each feature space direction. A large sum in the coefficient results in slowing down diffusion, encouraging point stability, while a small sum accelerating diffusion, causing rapid movement of the points.

The value of $\varepsilon(e_{uv})$ in the diffusion coefficient depends on the type of diffusion. For forward diffusion, $\varepsilon(e_{uv})$ is a positive constant, fostering clustering. Contrarily, backward diffusion uses a small negative $\varepsilon(e_{uv})$, causing repulsion between different clusters. This forward-backward diffusion combination allows for supervised learning.

The basic model behaviour can be described on points divided into clusters. Points inside a cluster are attracted by forward diffusion, which means that only forward diffusion is applied to the edges connecting the points from the same cluster. On the edges connecting the points from different clusters, backwards diffusion is applied, thus, different clusters repel through backward diffusion. Moreover, when a new observation is added to the network, only forward diffusion is applied to links affecting the new vertex, attracting it to existing clusters. The network dynamics determine the cluster membership of the new observation.

To reduce the influence of forward diffusion on a new observation $w \in V(G)$, the diffusion coefficient can be modified as:

$$g(e_{vw}) = \max(\varepsilon(e_{vw}) \frac{1}{1 + \sum_{i=1}^{k} (K_i \; l_i^2(e_{vw}))} - \delta, \; 0), \; \varepsilon(e_{vw}) > 0, \tag{2.3}$$

where δ controls the "diffusion neighbourhood," restricting attraction only to points with sufficiently large diffusion coefficients.

To discretise equation (2.1), we utilise *i)* the balance of diffusion fluxes (inflows and outflows) at each vertex $v \in V(G)$ and *ii)* the approximation of diffusion fluxes towards vertex v along its edges.

We introduce the diffusion flux approximation, depending on the difference in function values X at vertices v and u, as

$$\mathcal{X}(v, e_{uv}, t) = g_{e_{uv}}(X(u,t) - X(v,t)), \tag{2.4}$$

for each directed edge e_{uv}, where $g_{e_{uv}}$ denotes the diffusion coefficient on edge e_{uv}. Positive $\mathcal{X}(v, e_{uv}, t)$ represents diffusion inflow, while negative $\mathcal{X}(v, e_{uv}, t)$ indicates outflow. The diffusion flux balance at vertex v is then expressed as

$$\partial_t X(v,t) = \sum_{\substack{u \in V(G) \ : \\ e_{uv} \in A(G)}} \mathcal{X}(v, e_{uv}, t). \tag{2.5}$$

Substituting the diffusion flux approximation (2.4) into the balance equation (2.5) results in the discrete version of graph PDE (2.1):

$$\partial_t X(v,t) = \sum_{\substack{u \in V(G) \ : \\ e_{uv} \in A(G)}} g_{e_{uv}}(X(u,t) - X(v,t)), \tag{2.6}$$

for more details see [8].

If $g_{e_{uv}} = 1$ and $\mathcal{X}(v, e_{uv}) = \frac{(X(u) - X(v))}{d_{e_{uv}}}$, where $d_{e_{uv}}$ is a distance between vertices v and u, then the sum on the right hand side of (2.5) is called graph-Laplacian. It is expressed by the following formula

$$\Delta X(v) = \sum_{\substack{u \in V(G) \ : \\ e_{uv} \in A(G)}} \frac{(X(u) - X(v))}{d_{e_{uv}}}. \tag{2.7}$$

Let us note that we do not consider $d_{e_{uv}}$ in the denominator in (2.6) because the distance of vertices v and u is included in diffusion coefficient $g_{e_{uv}}$ and its influence is thus already taken into account. However, the definition (2.7) is important and will be used in the next section for graph-Laplacian of image intensity.

For time discretisation of (2.6), we use the semi-implicit approach [10], utilising finite difference for time derivative approximation. Due to time-dependent changes in diffusion coefficient $g_{e_{uv}}$ (refer to (2.2) and (2.3)), we take its value from the previous time step. For data classification in k-dimensional feature space, each time step yields k systems of linear equations

$$(1 + \tau \sum_{\substack{u \in V(G) \ : \\ e_{uv} \in A(G)}} g^{n-1}_{e_{uv}}) x_i^n(v) - \tau \sum_{\substack{u \in V(G) \ : \\ e_{uv} \in A(G)}} g^{n-1}_{e_{uv}} x_i^n(u) = x_i^{n-1}(v), \tag{2.8}$$
$$i = 1, \ldots, k, \quad v \in V(G),$$

interconnected by diffusion coefficient $g^{n-1}_{e_{uv}}$, depending on all $x_i^{n-1}(v)$, $x_i^{n-1}(u)$, $i = 1, \ldots, k$, given by

$$g^{n-1}_{e_{uv}} = \varepsilon(e^{n-1}_{uv}) \frac{1}{1 + \sum_{i=1}^{k} (K_i \ l_i^2(e^{n-1}_{uv}))}, \qquad K_i \geq 0. \tag{2.9}$$

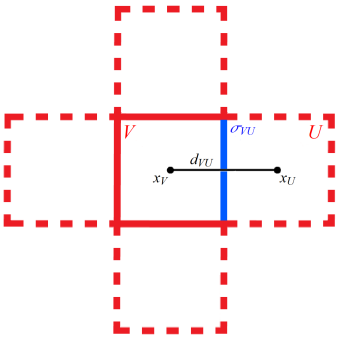

FIG. 3.1. *A motivation for definition of the Laplace operator on the graph. For a detailed description of the figure see equation (3.1).*

The equations (2.8)-(2.9) represent basic NatNet dynamics, where points in clusters move together while clusters themselves repulse. The addition of a new observation alters this dynamic. For a new observation w, the diffusion coefficient (2.9) is modified to

$$g_{e_{uw}}^{n-1} = \max(\varepsilon(e_{uw}^{n-1}) \frac{1}{1 + \sum_{i=1}^{k} (K_i \; l_i^2(e_{uw}^{n-1}))} - \delta, \; 0), \tag{2.10}$$

where $\varepsilon(e_{uw}^{n-1}) > 0, \; K_i \geq 0, \; \delta > 0$ are given constants, see also (2.3).

3. The Graph-Laplacian for images. Let us consider a scalar function $f(x)$ defined over a bounded domain $\Omega \subset R^2$, where $x \in \Omega$ denotes a point in this domain. The Laplace operator Δf provides a measure of the local variation of $f(x)$ across the domain. In the context of image processing, understanding the behaviour of the Laplacian across its pixels is crucial for our task.

The mean value of the Laplacian in a finite volume (pixel) V, see Fig. 3.1, can be expressed by applying Green's theorem in terms of the gradient of the function $f(x)$ and the normal vector to the boundary of V:

$$\begin{aligned} \frac{1}{m(V)} \int_V \Delta f \; dx &= \frac{1}{m(V)} \int_{\partial V} \nabla f \cdot \vec{n} \; dS \; \approx \\ &\approx \frac{1}{m(V)} \sum_{U \in \mathcal{N}(V)} m(\sigma_{VU}) \frac{f(x_U) - f(x_V)}{d_{VU}}, \end{aligned} \tag{3.1}$$

where $m(V)$ denotes the 2D measure of the finite volume V, ∂V represents the boundary of V, and $\vec{n}$ is the unit outer normal to ∂V. The $\mathcal{N}(V)$ is the set of neighbouring finite volumes U for which the 1D measure of the common face $m(\sigma_{VU})$ is nonzero, and d_{VU} is the length of the line connecting the centres x_V and x_U of finite volumes V and U.

Inspired by the physical Laplacian given by the formula (3.1), the graph-Laplacian is defined by (2.7) in the previous section. Instead of finite volume V we consider vertex v of the graph G and its neighbouring vertices u connected with v by an edge e_{vu}. The equation (2.7) generalises the notion of the Laplace operator from physical applications to the more general topological structures such as graphs, enabling its application to data represented as networks. When working with images, we can

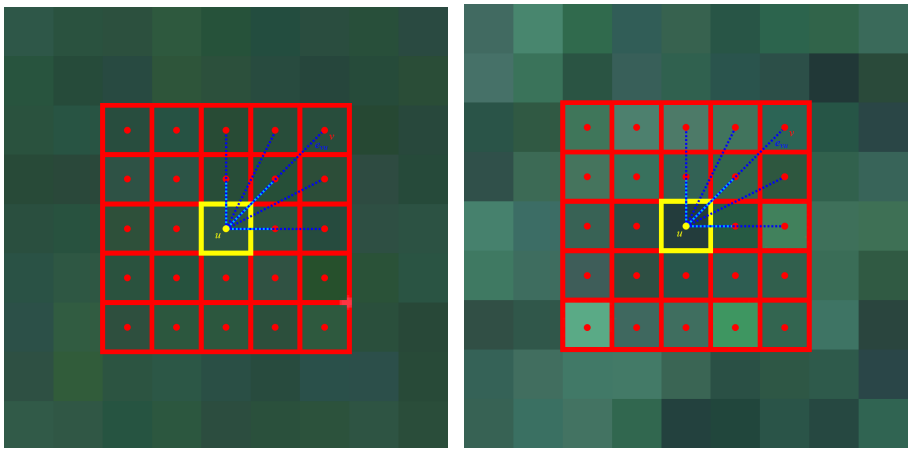

FIG. 3.2. *Examples of* 5×5 *neighbourhood (red squares) for the graph-Laplacian calculation in the examined pixel (yellow square) and some edges connecting examined pixel represented vertex* v *with neighbouring pixels/ vertices* u*. On the left, the resulting graph-Laplacian value is* 27.64 *because the function of the image intensity of the green channel is smooth. On the right, it is* 701.88*, because the function of the image intensity of the green channel has more extremes.*

consider a squared neighbourhood of the pixel and consider the pixels in such neighbourhood as vertices of the graph connected by the edges. The examples of the squared neighbourhood are depicted in Fig. 3.2, where the yellow square represents vertex v and the red squares represent the neighbouring vertices u. Some edges in light blue and dotted dark blue colour connecting the vertices are also depicted in Fig. 3.2. If we denote image intensity as f we can rewrite its graph-Laplacian into the form

$$\begin{aligned} \Delta f(v) &= \sum_{\substack{u \in V(G) \\ e_{vu} \in E(G)}} a_{vu}(f(u) - f(v)) \\ &= \sum_{\substack{u \in V(G) \\ e_{vu} \in E(G)}} a_{vu}\ f(u) - \sum_{\substack{u \in V(G) \\ e_{vu} \in E(G)}} a_{vu}\ f(v), \end{aligned} \tag{3.2}$$

where $a_{vu} = \frac{1}{d_{vu}}$ is a weight by which the values of $f(u)$ in neighbouring vertices are multiplied while the value $f(v)$ is multiplied by the sum of all the weights with the minus sign and d_{vu} is the distance between vertices v and u. In our application, we consider 5×5 pixel neighbourhood centred in the vertex (pixel) v, considering all other pixels in such neighbourhood as vertices u. Then we get the matrix of the weights multiplying the image intensities in the 5×5 neighbourhood as follows

$$\begin{bmatrix} \frac{1}{\sqrt{8}} & \frac{1}{\sqrt{5}} & \frac{1}{2} & \frac{1}{\sqrt{5}} & \frac{1}{\sqrt{8}} \\ \frac{1}{\sqrt{5}} & \frac{1}{\sqrt{2}} & 1 & \frac{1}{\sqrt{2}} & \frac{1}{\sqrt{5}} \\ \frac{1}{2} & 1 & - \sum_{\substack{u \in V(G) \\ e_{vu} \in E(G)}} a_{vu} & 1 & \frac{1}{2} \\ \frac{1}{\sqrt{5}} & \frac{1}{\sqrt{2}} & 1 & \frac{1}{\sqrt{2}} & \frac{1}{\sqrt{5}} \\ \frac{1}{\sqrt{8}} & \frac{1}{\sqrt{5}} & \frac{1}{2} & \frac{1}{\sqrt{5}} & \frac{1}{\sqrt{8}} \end{bmatrix}. \tag{3.3}$$

The graph-Laplacian concept can capture image variability, which is reflected in its values. In the areas where the image intensity has many local extrema, the values

of the graph-Laplacian should be higher. Meanwhile, we will obtain lower values for graph-Laplacian in the areas with more uniform image intensity.

4. Numerical experiments. The following section explores the possibility of applying graph-Laplacian. Two methodologies are examined, where the graph- Laplacian combined with relevancy maps, or graph-Laplacian as part of the feature space for NatNet.

4.1. Graph-Laplacian combined with relevancy maps. In the first numerical experiment, we combine the aforementioned graph-Laplacian given by the (3.2) with the relevancy map constructed by the trained NatNet. First, let us apply the weight mask (3.3) to each pixel of the Sentinel-2 image. The Sentinel-2 European Space Agency satellite produces the imagery in the 13 optical bands [5]. In this experiment, we focus only on the band with $559nm$, which is a green colour in the spectrum. Subsequently, we compute the absolute value of the graph-Laplacian in each image pixel and normalise it to the interval $[0, 1]$.

The highest values of the graph-Laplacian occur in urban areas, attributed to the presence of diverse structures such as buildings, streets, and parks in a relatively small space. When attempting to differentiate between natural and planted forests, this led to reduced accuracy as the high graph-Laplacian values in urban areas diminish the contrast between graph-Laplacian values in natural and planted forests. It becomes obvious that urban areas, and more broadly, any areas not corresponding to natural forest habitats, must be excluded from the analysis. To achieve this, we utilise a relevancy map generated by the Natural Numerical Network for the classification of the riparian forest habitats.

The relevancy map, a grayscale image of the same dimensions as the Sentinel-2 image, highlights forested areas of the target habitat in pixels with a white colour, where the relevancy acquires values close to 1. Non-habitat areas such as fields, rivers, and cities appear black on the relevancy map, which means that the relevancy of the appearance of the target habitat is close to 0. The pixels acquire a grey colour on the relevancy map when the relevancy of the appearance of the target forest habitat has a value between 0 and 1 (the colour in the pixels is darker grey when the relevancy is closer to 0). The calculation of the relevancy coefficient of the appearance of the target forest habitat and construction of the relevancy maps are in detail described in the [8]. As depicted in the first row of Fig. 4.1, the alluvial areas of the Danube River are shown on the Sentinel-2 image on the left, while the relevancy map for the riparian forest from the Danube River alluvial areas is displayed on the right. Additionally, segmented regions denoting natural riparian forests (yellow curves) and planted riparian forests (red curves), provided by botany experts from the Plant Science and Biodiversity Centre SAS using semi-automatic and automatic segmentation methods [12, 11], are illustrated in all subfigures of Fig. 4.1. One can see that the interior of the yellow segmented areas exhibits white colours, indicating high relevancy for the riparian forest habitat. However, we also observe white colours in the interior of the red segmented areas, suggesting that these areas are potential candidates for the riparian forest due to the similar species composition of natural and planted riparian forests. Since these areas are not natural, they must be excluded from the Natura 2000 habitat identification.

Based on these observations, we propose a methodology that combines the relevancy map with the mean value of graph-Laplacian (3.2) calculated in a $m \times m$ neighbourhood centred at the examined pixel.

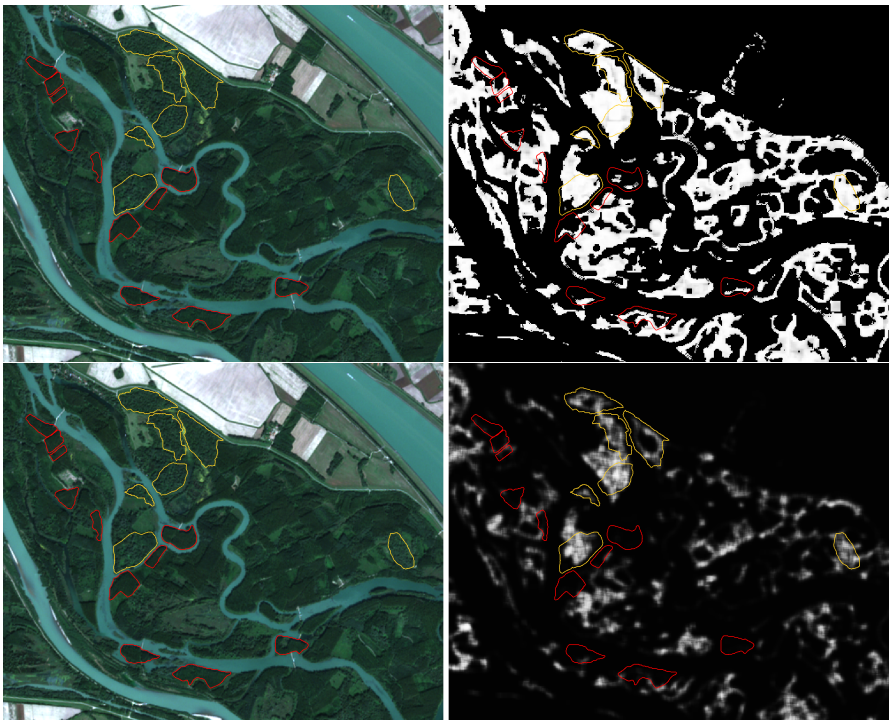

FIG. 4.1. *The comparison of the relevancy map created by the Natural Numerical Network (upper row) and the Mean graph-Laplacian map (bottom row). The upper left and bottom left images depict the Sentinel-2 image. The upper right image shows the relevancy map $R(p)$, and the bottom right image shows the Mean graph-Laplacian map $M(p)$. The images also depict segmented areas of natural forests (yellow segmented areas) and planted forests (red segmented areas).*

- First, we calculate the relevancy map $R(p)$ for riparian forest habitat, where p is the examined pixel in the desired location as described in [8].
- Then, we set the graph-Laplacian value computed by (3.2) for all pixels p for which $R(p) \neq 0$, for other pixels we set the value to 0.
- Finally, the Mean graph-Laplacian map $M(p)$ is created: to every pixel p, for which $R(p) \neq 0$, we set the mean value of graph-Laplacian in the neighbourhood $m = 7$, and we set 0 value otherwise.

The Mean graph-Laplacian map $M(p)$ is depicted in the bottom right subfigure of Fig. 4.1. Comparing two relevancy maps, the Mean graph-Laplacian map $M(p)$ shows a significant reduction of the high values of the relevancy for planted forests in comparison with the relevancy map $R(p)$. By application of the mean graph-Laplacian, the values are either zero or very low in such areas, indicating considerable success in capturing low biodiversity. Consequently, the interior of the red segmented areas has a colour close to black. Contrarily, the mean graph-Laplacian effectively captures the variability of the image intensity in the natural forests, with high values in the interior of the yellow segmented areas, indicating substantial biodiversity in those regions.

4.2. Graph-Laplacian as a feature in NatNet. In the second numerical experiment, the graph-Laplacian operator is used as a statistical characteristic in the construction of NatNet feature space. In [8, 9], the feature space was calculated

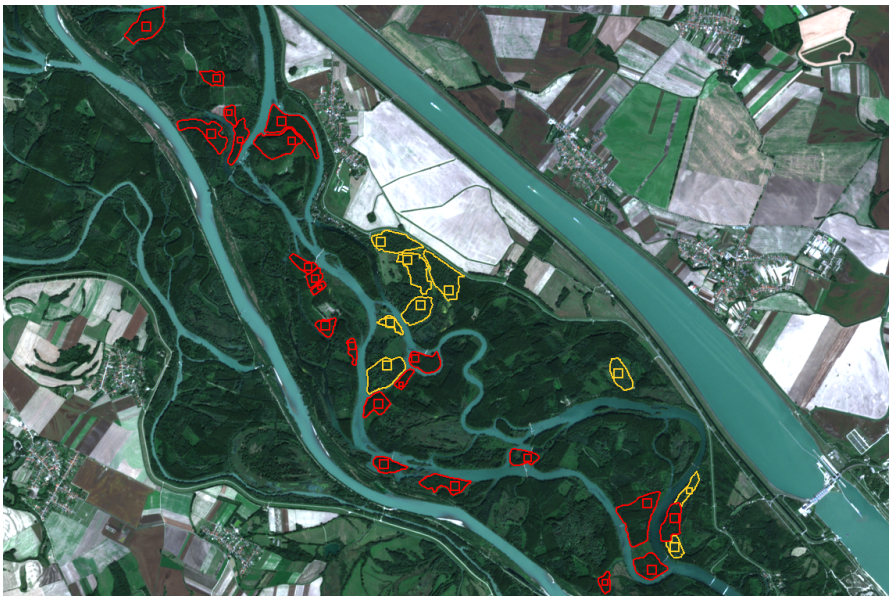

FIG. 4.2. *The subregion of Western Slovakia with segmented areas of Natura 2000 riparian forest habitat (yellow curves) and planted monodominant forests (red curves). Together with the segmented areas, representative squares are also plotted inside the segmented areas.*

using statistical characteristics such as mean, standard deviation, and minimal and maximal values in the representative squares of the segmented areas. The following experiment aims to evaluate the efficiency of the graph-Laplacian operator as the statistical characteristic and its impact on classification outcomes.

A dataset including segmented areas of natural and planted forests is constructed to achieve this objective. The graph-Laplacian is computed by applying the prescribed weight mask (3.3) to interior pixels in each desired area from all channels of the Sentinel-2 satellite imagery. Because the segmented areas do not have the same number of pixels, the representative squares of the size $n = 7, 9, 11$ are constructed inside the segmented areas as depicted in Fig 4.2. Then, the mean graph-Laplacian is calculated in representative squares in each desired area. It gives the feature vectors forming vertices of the NatNet directed graph. This directed graph represents the initial position of the vertices for subsequent training processes of the NatNet described in [8]. Notably, the training effectiveness is significantly high, achieving a success rate of 100%, which enables the utilisation of the trained NatNets for generating relevancy maps $Q(p)$, where p is the pixel.

The methodology to use trained NatNet, which used the graph-Laplacian of each channel of Sentinel-2, is proposed, and the goal is to highlight biodiversity hotspots, the natural forests with a high biodiversity value. When we properly combine the relevancy map $R(p)$ calculated for the riparian forest habitat with the relevancy map $Q(p)$ computed by using the graph-Laplacian, we can achieve that goal:

- First, the relevancy map $R(p)$ for the riparian forest habitat is computed. Given that the dominant species in the riparian forest habitat often coincide with those dominant in planted riparian forests, the relevancy map also highlights regions planted by commercially used riparian forests. This aspect is shown in Fig. 4.3 upper right.

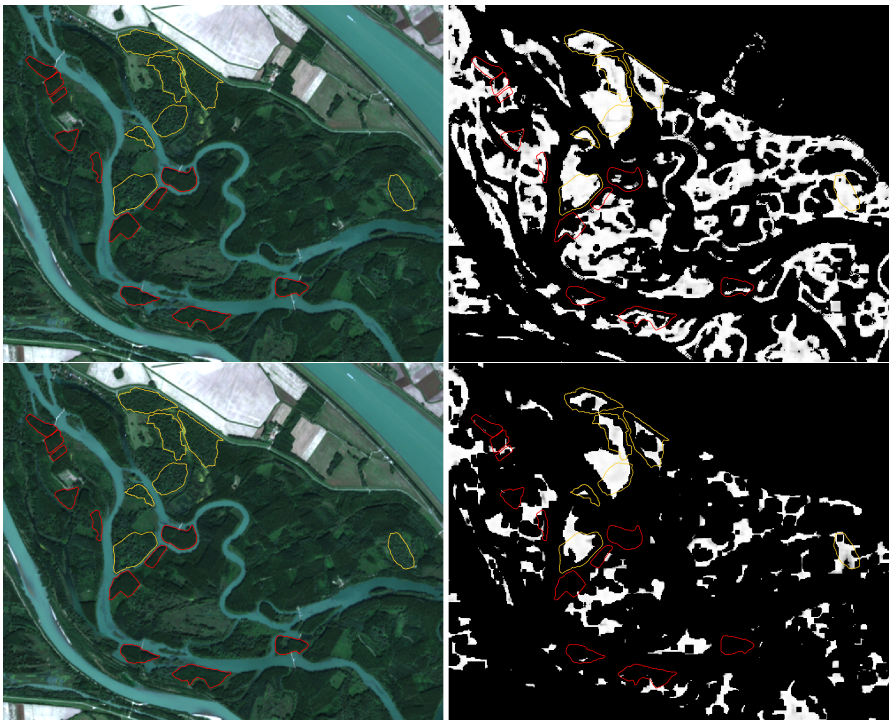

FIG. 4.3. *The comparison of the relevancy map created by the Natural Numerical Network for the forested areas in the target habitat (upper right) and the relevancy map highlighting the biodiversity hotspots of the target habitat(bottom right). The upper left and bottom left images depict the Sentinel-2 image. The images also depict segmented areas of natural forests (yellow segmented areas) and planted forests (red segmented areas).*

- To model the possible areas of the biodiversity hotspots, planted forests, and the transitive zones between natural habitats and other types of land coverage have to be excluded. Then, the squared neighbourhood of size 5×5 centred in every pixel p in relevancy map $R(p)$ is constructed, and the values in the pixels inside the squares are studied.
- Suppose we found at least one pixel with a zero value in the relevancy map $R(p)$ inside the constructed square around pixel p. In that pixel p, the value of the new grayscale Hotspots map $H(p) = 0$.
- If there are no pixels with zero values inside the square in the relevancy map $R(p)$, we set $H(p) = Q(p)$.

Such a process leads to the construction of the grayscale Hotspots map $H(p)$ depicted in Fig. 4.3 bottom right, where we can observe a reduction of the high value of the relevancy and only a few white parts highlighting the biodiversity hotspots remained. This result demonstrates the success in effectively indicating biodiversity hotspots of natural forests in the target habitat using the graph-Laplacian of Sentinel-2 optical bands in NatNet.

5. Conclusions. This study demonstrates the potential of the graph-Laplacian operator in biodiversity modelling through its combination with Natural Numerical Networks. By extending the use of the Laplace operator to graph structures, the proposed methodology effectively captures local variations and structural properties

in ecological data. This approach enhances the accuracy of identifying and classifying natural riparian forests with high biodiversity from satellite imagery. The application of the graph-Laplacian as a statistical characteristic in the NatNet allows for differentiation between natural and planted forests. The experimental results confirm the usability of this method in highlighting biodiversity hotspots and its practical utility in environmental science, specifically in the context of protected habitat identification under the Natura 2000 network. The next step is to analyse graph-Laplacian values in the interior pixels of the segmented areas and construct the quantity Relative High graph-Laplacian, which will capture the diversity locally in segmented areas. This information makes it possible to distinguish if the examined areas are natural forests with a high value of Relative High graph-Laplacian. In the case of the planted forests, the Relative High graph-Laplacian value should be low.

REFERENCES

[1] Bang-Jensen, J., Gutin, G.R.: Digraphs: Theory, Algorithms and Applications. Springer-Verlag London, 2st edn. (2010)

[2] Böhm, J.N., Berens, P., Kobak, D.: Attraction-repulsion spectrum in neighbor embeddings. Journal of Machine Learning Research **23**(95), 1–32 (2022)

[3] Chang, B., Meng, L., Haber, E., Ruthotto, L., Begert, D., Holtham, E.: Reversible architectures for arbitrarily deep residual neural networks. In: 32nd AAAI Conference on Artificial Intelligence, AAAI 2018. vol. 32, pp. 2811–2818 (04 2018), `https://ojs.aaai.org/index.php/AAAI/article/view/11668`

[4] European Environmental Agency: The natura 2000 protected areas network. `https://www.eea.europa.eu/themes/biodiversity/natura-2000/the-natura-2000-protected-areas-network` (2024)

[5] European Space Agency: Sentinel 2. `https://sentinel.esa.int/web/sentinel/missions/sentinel-2` (2024)

[6] Friedman, J., Tillich, J.P.: Calculus on graphs. CoRR **cs.DM/0408028** (2004)

[7] Haber, E., Ruthotto, L.: Stable architectures for deep neural networks. Inverse Problems **34**(1) (2018). https://doi.org/10.1088/1361-6420/aa9a90

[8] Mikula, K., Kollár, M., Ožvat, A.A., Ambroz, M., Čahojová, L., Jarolímek, I., Šibík, J., Šibíková, M.: Natural numerical networks for natura 2000 habitats classification by satellite images. Applied Mathematical Modelling **116**, 209–235 (2023). https://doi.org/10.1016/j.apm.2022.11.021

[9] Mikula, K., Kollár, M., Ožvat, A.A., Čahojová, L., Šibíková, M.: Natural numerical networks on directed graphs in satellite image classification. Scale Space and Variational Methods in Computer Vision **14009**, 339–351 (2023). https://doi.org/10.1007/978-3-031-31975-4

[10] Mikula, K., Ramarosy, N.: Semi-implicit finite volume scheme for solving nonlinear diffusion equations in image processing. Numerische Mathematik **89**(3), 561–590 (2001)

[11] Mikula, K., Urbán, J., Kollár, M., Ambroz, M., Jarolímek, I., Šibik, J., Šibíková, M.: An automated segmentation of natura 2000 habitats from sentinel-2 optical data. Discrete and Continuous Dynamical Systems - Series S **14**(3), 1017–1032 (2021). https://doi.org/10.3934/dcdss.2020348

[12] Mikula, K., Urbán, J., Kollár, M., Ambroz, M., Jarolímek, I., Šibik, J., Šibíková, M.: Semi-automatic segmentation of natura 2000 habitats in sentinel-2 satellite images by evolving open curves. Discrete and Continuous Dynamical Systems - Series S **14**(3), 1033–1046 (2021). https://doi.org/10.3934/dcdss.2020231